Science of the Total Environment 842 (2022) 156923

Contents lists available at ScienceDirect

Science of the Total Environment

journal homepage: www.elsevier.com/locate/scitotenv

Antagonistic *in vivo* interaction of polystyrene nanoplastics and silver compounds. A study using *Drosophila*

Mohamed Alaraby [a,b], Doaa Abass [a,b], Aliro Villacorta [a,c], Alba Hernández [a], Ricard Marcos [a,*]

[a] Group of Mutagenesis, Department of Genetics and Microbiology, Faculty of Biosciences, Universitat Autònoma de Barcelona, Campus of Bellaterra, 08193 Cerdanyola del Vallès, Barcelona, Spain
[b] Zoology Department, Faculty of Sciences, Sohag University, 82524 Sohag, Egypt
[c] Facultad de Recursos Naturales Renovables, Universidad Arturo Prat, Iquique, Chile

HIGHLIGHTS

- The potential interaction between nanopolystyrene and silver was evaluated in *Drosophila*.
- The coexposure increased the silver internalization regarding silver exposure alone.
- TEM + EDX analysis showed the absorption of silver compounds by nanopolystyrene.
- Coexposure reduces the levels of oxidative stress and genotoxicity, regarding silver effects.
- The antagonistic interaction could be due to the reduced bioavailability of silver once absorbed by polystyrene.

GRAPHICAL ABSTRACT

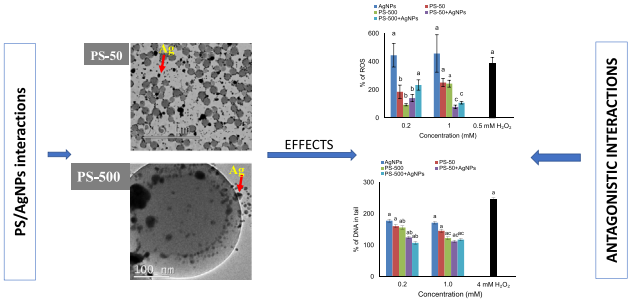

Polystyrene MNPLs confine silver, reducing its oxidative and genotoxic impacts

ARTICLE INFO

Editor: Damià Barceló

Keywords:
Nanoplastics
Polystyrene
Silver nanoparticles
Carriers
Size
Uptake
Oxidative stress
Genotoxicity
Antagonistic interaction
Drosophila melanogaster

ABSTRACT

Since heavy metals and micro − /nanoplastics (MNPLs) can share common environmental niches, their potential interactions could modulate their hazard impacts. The current study was planned to evaluate the potential interactions between silver compounds (silver nanoparticles or silver nitrate) and two different sizes of polystyrene nanoplastics (PSNPLs) (PS-50 and PS-500 nm), administered *via* ingestion to *Drosophila* larvae. While egg-to-adult survival was not affected by the exposure to silver compounds, PSNPLs, or their coexposures, the combined treatments succeeded to restore the delay of fly emergence induced by silver compounds. Transmission electron microscopy (TEM) and inductively coupled plasma mass spectrometry (ICP-MS) showed the ability of PSNPLs to transport silver compounds (regardless of their form) across the intestinal barrier, delivering them into the hemolymph of *Drosophila* larvae in a concentration exceeding that mediated by the exposure to silver compounds alone. The molecular response (gene expression) of *Drosophila* larvae greatly fluctuated, accordingly if exposures were administered alone or in combination. Although PSNPLs produced some oxidative stress in the hemocytes of *Drosophila*, especially at the highest dose (1 mM), higher levels were observed after silver exposure, regardless of its form. Interestingly, the oxidative stress of silver, especially that produced by nano-silver, drastically decreased when coexposed with PSNPLs. Similar effects were observed regarding the DNA damage induced in *Drosophila* hemocytes, where cotreatment decreased the genotoxicity induced by silver compounds. This antagonistic interaction could be attributed to the ability of tiny plastic specks to confine silver, avoiding its bioavailability, and diminishing their potential impacts.

* Corresponding author at: Grup de Mutagènesi, Departament de Genètica i de Microbiologia, Facultat de Biociències, Universitat Autònoma de Barcelona, Campus de Bellaterra, 08193 Cerdanyola del Vallès, Barcelona, Spain.
E-mail addresses: mohamed.alaraby@science.sohag.edu.eg (M. Alaraby), ricard.marcos@uab.es (R. Marcos).

http://dx.doi.org/10.1016/j.scitotenv.2022.156923
Received 8 April 2022; Received in revised form 27 May 2022; Accepted 20 June 2022
Available online 23 June 2022

1. Introduction

The increasing levels of micro/nanoplastics (MNPLS) in our environment arise many questions about their potential hazards. Its consideration as contaminants of emergent concern requires generating scientifically sound data to understand the potential health risks associated with their exposure (Mitrano et al., 2021). Although microplastics were environmentally detected early in 1990 (Ryan and Moloney, 1990), their extensive research skyrocketed recently (Bhagat et al., 2021) and, among the different questions raised by the environmental presence of MNPLs, their possible interactions with other environmental pollutants stand out.

It has been reported that MNPLs can act as sponge adsorbing pathogens (Viršek et al., 2017), pharmaceuticals (Razanajatovo et al., 2018), pesticides (Fajardo et al., 2022), and heavy metals (Zhou et al., 2020; Khalid et al., 2021), among others compounds. This would be a consequence of their large surface area and hydrophobicity (Bhagat et al., 2021). Regarding heavy metals, they are major contaminants of soil and water (Zhou et al., 2020) and, consequently they share environmental niches with environmental MNPLs. Nevertheless, limited knowledge is available on their interactions, as well as on the biological impacts resulting from their combined exposures (Cao et al., 2021). The interactions between metals-plastics can induce substantial changes to the physicochemical properties of plastics, altering their internalization and accumulation in the exposed organisms (Hansjosten et al., 2022). Moreover, the mechanisms controlling the adsorption mechanisms are not completely specified (Liu et al., 2022) whether they are synergistic (Qiao et al., 2019; Lee et al., 2019), additive (Ma et al., 2016), or antagonistic (Oliveira et al., 2018).

The interaction between MNPLs and environmental pollutants (including heavy metals) can be modulated by different physicochemical parameters, and also by the MNPLs size. Differences in size between MPLs and NPLs can also modulate their interaction with environmental pollutants due to differences in surface area, bioavailability, and adsorption efficiency (Gigault et al., 2021). Due to the technical difficulties of detecting/quantifying NPLs in environmental matrices, most environmental studies have used MPLs as a model of MNPLs. Nevertheless, the small size of NPLs makes easier their uptake by the organisms and, consequently, they could become more hazardous. For this reason, studies using NPLs are usually carried out in laboratory conditions and using both *in vitro* and *in vivo* approaches. Studies using whole organisms can produce data more useful to be extrapolated for risk assessment approaches.

Nevertheless, most of the *in vivo* studies aiming to detect potential interactions MNPLs/ environmental pollutants focus on aquatic animals, mainly because marine MNPLs are considered to act as very important vectors of many marine pollutants (Amelia et al., 2021). Nevertheless, MNPLs are widely spread in all environmental niches including also continental waters, air, and soils. This would mean that other *in vivo* models, out of the aquatic organisms, should also be used/explored. In that context, *Drosophila* stands out as a powerful *in vivo* model to determine the potential hazards induced by environmental nanoparticles, including nanoplastics (Alaraby et al., 2016a, 2021).

Using *Drosophila* as an *in vivo* experimental model our aim is to evaluate potential interactions between polystyrene nanoplastics (PSNPLs), used as a model of nanoplastic, and silver as a model of metal pollutant. Although when thinking about MNPLs pollutants we imagine those resulting from the degradation of plastic goods (secondary MNNPLs), MNPLs are also created at these sizes for specific purposes (primary MNPLs). Thus, for example, polystyrene micro and nanobeads are created/used for different purposes like for the exfoliating agents present in personal care products such as creams, and toothpaste, among other uses (Silva et al., 2018). Nevertheless, independently of their origin, as primary or secondary MNPLs, all finally are present in the different environmental compartments as environmental pollutants. The antibacterial activity and the high electrical and thermal conductivity of silver compounds have extended their use in many fields including catalysts, cosmetics, electronics, and textiles. Consequently, they are polluting many environments, including aquatic ones, and are present in the respective sediments (Zhao et al., 2021).

Since silver materials and MNPLs can share a common environment, some types of interactions can take place (Bhagat et al., 2021). Therefore, our aim is to investigate the potential interactions between two different sizes of polystyrene nanoplastics (50 and 500 nm) and two silver compounds as silver nanoparticles (AgNPs, about 10 nm) and silver nitrate (as a source of silver ions). To detect such interactions, we have used *Drosophila melanogaster* to evaluate a wide range of effects including uptake and toxicity, as well as changes in the expression of genes involved in different functional pathways, oxidative stress, and genotoxicity. It is important to indicate that we have previously described the physical interaction between AgNPs and PSNPLs, as well as their biological effects using human intestinal Caco-2 cells (Domenech et al., 2021). In addition, we have successfully used the *Drosophila* larvae as a useful *in vivo* model to determine the effect of the ingested nanomaterials and their effects on the intestinal components (Alaraby et al., 2018).

2. Materials and methods

2.1. Silver and polystyrene nanoparticles characterization

AgNPs were purchased from nanoComposix (San Diego, CA, USA), with standard properties according to the manufacturer (diameter: 6.6 ± 1.8 nm; surface area: 76.1 m^2/g; solvent: USP purified water). Two different sizes of polystyrene nanoparticles (PSNPLs) were obtained from Spherotech (Lake Forest, IL, USA), PS-50 (80 nm; reference SPH-PP-008-10), and PS-500 (430 nm, reference SPH-PP-05-10). According to the manufacturer the PSNPLs were prepared through polymerization of styrene monomer using potassium persulfate as a polymerization initiator, resuspended in deionized water, and sodium azide (0.02 %) was added as a bacteriostatic. The other chemicals, including $AgNO_3$ (ref. 209,139), were from Sigma Chemical Co. (St. Louis, MO, USA). To further characterize AgNPs and PSNPLs, a Malvern Zetasizer Nano-ZS zen3600 instrument (Malvern, UK) was used to determine the hydrodynamic size and the zeta potential; transmission electron microscopy (TEM; Jeol 1400; Jeol Ltd., Tokyo, Japan) was used to show size, morphology, and degree of aggregation; energy-dispersive X-ray spectroscopy (EDX) spectrum was used to evaluate the sorption of silver particles upon polystyrene using a TEM (200 kV) Jeol 2011 device (Jeol Ltd., Tokyo, Japan). The functional groups of polystyrene were determined by Fourier-transform infrared spectroscopy (FTIR) using a Hyperion 2000 micro-spectrometer (Bruker, Billerica MA, USA). This analysis was carried out at the Molecular Spectroscopy and Optical Microscopy facility at the *Institut Català de Nanociència i Nanotecnologia* (ICN2). To assess the composition, interferograms were analyzed and contrasted with previous reports. To achieve the desired concentrations, PSNPLs were dispersed in Mili-Q water.

2.2. Drosophila melanogaster exposure

The wild-type Canton-S strain was used for all experiments. The experimental design includes treatments of *Drosophila* with two different concentrations of silver compounds (AgNPs and $AgNO_3$) and two of PSNPLs (PS-50 and PS-500) alone, or with the different combinations (i) AgNPs + PS-50, (ii) AgNPs + PS-500, (iii) $AgNO_3$ + PS-50, (iv) $AgNO_3$ + PS-500. Two exposure scenarios were established, (i) a low exposure where 0.2 mM of all the components were used, and (ii) a high exposure where 1 mM was used. The equivalent concentrations of 0.2 and 1 mM for nanopolystyrene correspond to 52 and 260 μg/g food; for silver NPs they correspond to 54 and 270 μg/g food; and for silver nitrate they correspond to 85 and 425 μg/g food. Stock solutions were freshly prepared before the experiments and diluted to prepare all proposed doses. Particle suspensions were vortexed before treatments to obtain an optimum distribution of nanoparticles. The chosen concentrations were based on the reported by us in previous studies (Alaraby et al., 2019, 2022).

2.3. Toxicity

Toxicity was evaluated according to the ability to move from egg to adult stages. To proceed, five replicates of groups of 50 eggs of Canton-S flies were seeded in food vials containing 4 g of instant medium (Carolina Biological Supply, Burlington, NC, USA), previously wetted with 10 mL of various concentrations (0.0, 0.2, and 1 mM) of silver ($AgNPs/AgNO_3$), or PSNPLs (PS-50/PS-500) whether alone or in combination. Vials were left at 25 °C, 60 % humidity, and (12 h/12 h light/dark) conditions. MiliQ water was used as a control solution. The vials were checked daily till adult emergence to check for any differences in the development of treated flies. The emerged adults were collected, investigated, and counted to establish comparisons with the untreated adults. Moreover, adults were investigated to record any morphological abnormalities. According to the toxicity information, the concentrations to be used in the other experiments were decided.

2.4. AgNPs and PSNPLs internalization

This section is proposed to answer several questions regarding the ability of PSNPLs to penetrate the intestinal barrier, as well as their ability to transfer heavy metals into the organism. Thus, the whole intestinal journey of PSNPLs alone, or mixed with silver compounds, was highlighted using TEM; while inductively coupled plasma mass spectrometry (ICP-MS) was used to determine the larval body internalization. Furthermore, changes in the expression levels of genes related to "physical stress", as indicative of "intestinal damage" were also determined.

2.4.1. TEM investigation

Drosophila larvae at the fifth day of exposure were investigated to highlight the ability of MNPLs internalization, and the transferring of silver materials. The exposed larvae were carefully collected, cleaned, and dissected in phosphate buffer solution (PB; 0.1 M, pH 7.4). Drops of hemolymph samples were poured upon TEM grids and left for further investigation, while the extracted intestines were manipulated following our previous protocol (Alaraby et al., 2015). The intestine samples were directly immersed in a fixation solution for 2 h (1 % glutaraldehyde and 4 % paraformaldehyde, prepared in 0.15 M PB at pH 7.4), post-fixed in osmium tetroxide 1 % (*w/v*) containing 0.8 % (w/v) potassium hexacyanoferrate, and washed four times with deionized water and sequential dehydration in acetone at 4 °C. Eponate 12™ resin (Ted Pella Inc., Redding, CA, USA) was used to embed the samples and polymerize them at 60 °C for 48 h. Next, semi-thin sections (1 μm thick) were cut with a Leica ultracut UCT microtome (Leica Microsystems GmbH, Wetzlar, Germany) and stained with 1 % (*w/v*) toluidine blue to select the proper areas of the intestine. Ultimately, ultrathin sections (100 nm in thickness) were obtained *via* cutting the resin blocks with a diamond knife (45°, Diatome, Biel, Switzerland) and placed on non-coated 200 mesh copper grids and contrasted with uranyl acetate for 30 min, and Reynolds lead citrate for 5 min. TEM (Jeol 1400,100 kV) equipped with a CCD Gatan ES1000w Erlangshen Camera (Gatan Inc., Pleasanton, CA, USA) was used to rummage sections for Silver and polystyrene.

2.4.2. Internalization by ICPMS

This technique was proposed to evaluate if MNPLs act as heavy metal carriers, modulating their internalization, and also as an indirect approach to detect MNPLs' internalization *via* absorbing metals such as silver. Fifth-days treated larvae, in addition to untreated ones, were collected, carefully washed, and transferred into a new untreated instant food medium for 6 h, to clean their gastrointestinal tract' lumen from silver. Next, larvae were collected again and stored at −80 °C for further analysis. Three replicates of larval samples (50–100 mg) of each dose were digested in a microwave oven in an acidic solution of HNO_3/H_2O_2 (1:1) in a Teflon container. Inductively coupled plasma mass spectrometry (ICP-MS) in an Agilent, Model 7500ce device was used to measure silver content in each of the tested samples.

2.5. Alteration of gene expression levels

Exposure to xenobiotic agents could mediate changes at the molecular level, affecting the expression levels of genes involved in different pathways. Such effects correspond with their potential mode of action. To this end, a battery of gene markers representative of different pathways is included. As representative of general stress markers, the *Heat-shock-protein-70* (*Hsp70*, NM_169441.2) and the *Heat-shock-protein-83* (*Hsp83*, NM_001274433.1) were included; as representative of oxidative stress markers, the *Catalase* (*Cat*, NM_080483.3) and the *Cu, Zn Superoxide dismutase 2* (*Sod2*, NM_057577.3) were selected; as representative of intestinal genes stimulated by physical stress, the *Dual oxidase* (*Duox*, NM_001273039.1) and the *Prophenoloxidase 2* (*PPO2*, NM_136599.4) were chosen; finally, the *8-oxoG glycosylase1* (*Ogg1*, NM_132271.5) was selected as a DNA repair gene. Gene expression changes were determined as previously published (Alaraby et al., 2018). Briefly, 30 third-instar larvae (120 h-old) were homogenized in ice-cold TRIzol® Reagent (Invitrogen, Carlsbad, CA, USA) and manipulated according to the manufacturer protocol to obtain pure mRNA, which was asserted using RNase-free DNase I (DNA-freeTM kit; Ambion, Paisley, UK). The quantity of the obtained mRNA was determined using a Nanodrop device and converted into cDNA using the Transcriptor First Strand cDNA Synthesis Kit (Roche) protocol and stored at −20 °C. cDNA samples were amplified by real-time RT-PCR using a Light Cycler 480 (Roche, Basel, Switzerland). To prepare RT-PCR samples for each gene, 10 μL of reaction volume was used containing 4 μL of cDNA (10 ng/μL) mixed with 5 μL of SYBER Green mix, and 1 μL of 10 μM gene-specific primers (forward and reverse); the housekeeping β-actin was used as control. RT-PCR reaction conditions: pre-incubation for 5 min at 95 °C, 1 cycle, and the amplification was repeated 45 times (10 s at 95 °C, 15 s at 61 °C, 72 °C for 25 s).

2.6. Detection of oxidative stress induction

Drosophila larvae' hemocytes have been the cell model used to detect the potential oxidative stress induction with different exposure conditions. On the fifth day of exposure, larvae were collected, washed, and dissected. The hemolymph of untreated larvae was divided into two groups; the first group was used as negative control and the second group was treated with 0.5 mM H_2O_2 and used as the positive control. Hemolymph samples were treated with 5 μM 6-carboxy-2,7′-dichlorodihydro-fluorescein diacetate (DCFH-DA) and incubated for 30 min at 24 °C. The fluorescent hemocytes were detected by a fluorescent microscope with an excitation of 485 nm and an emission of 530 nm (green filter). The effects were quantified with the ImageJ program.

2.7. DNA damage induction

Hemocytes of larvae exposed to different conditions were used as cell models to detect DNA damage *via* the comet assay, according to our previously developed method (Alaraby et al., 2021). The 72 h-old larvae reared upon normal medium were collected, cleaned, and transferred into new vials containing instant medium, previously mixed with 10 mL of the different doses of the designed treatments. Nine exposure conditions were evaluated: AgNPs, $AgNO_3$, PS-50, PS-500, AgNPs + PS-50, AgNPs + PS-500, $AgNO_3$ + PS-50, $AgNO_3$ + PS-500, and 4 mM EMS as positive control, in addition to the negative control. Exposures last for 24 h and three replicates were carried out. Next, pooled larvae (50 larvae) of each treated group, were picked up and dissected in 100 μL of filtered and cold autoclaved phosphate buffer solution. To proceed, a sample of 10 μL of hemolymph containing about 10,000 cells was carefully mixed with 90 μL of 0.75 % low-melting agarose at 37 °C. Seven μL of hemocytes/agarose mixture (6 drops) were dropped on the hydrophilic surface of an ice-cold Gelbond®

film (GBF) (Life Sciences, Lithuania) in triplicate. To avoid artificial DNA damage, all next procedures were performed under dim light. The GBFs were submerged in freshly cooled lysis solution (2.5 M NaCl, 0.1 M Na_2EDTA, 0.2 M NaOH, 0.01 M Tris, 1 % Triton X-100, and 1 % N-lauryl sarcosinate, pH 10) for 1 h at 4 °C for cells lysis. The GBFs were washed for 5 min with cold electrophoresis buffer (0.001 M EDTA, 0.3 M NaOH, pH 13.2) before incubation for 25 min in a horizontal gel-electrophoresis tank, filled with cold electrophoresis buffer to permit unwinding DNA. Electrophoresis was directly performed for 20 min at conditions of 20 V and 300 mA at 4 °C. The GBFs were neutralized with two washes of PBS for 5 min each, followed by 1 min in distilled water, then fixed in absolute ethanol for at least 2 h, fixed for 5 min in 70 % and 100 % ethanol, respectively, then they air-dried for 2 h. The GBFs were stained with 25 mL of TE-buffer (10 mM Tris; 1 mM EDTA, pH 7.5) containing 1000× diluted SYBERGold fluorochrome for 20 min, with brief shaking, then washed with water to remove stain excess, and left to dry overnight. DNA damage of hemocytes was measured using the Komet 5.5 Image-Analysis System (Kinetic Imaging Ltd., Liverpool, UK) fitted with an Olympus BX50 fluorescence microscope equipped with a 480–550-nm wide-band excitation filter, and a 590-nm barrier filter. The percentage of DNA in the tail of the nucleoids was measured in three replicates of 100 randomly selected cells per dose, and compared with that of the negative control.

2.8. Statistical analysis

To address the normality and the homogeneity of the data the Kolmogorov-Smirnov & Shapiro-Wilk test and Levene's test were applied. The data showing normal distribution and equal variance were analyzed with the Student *t*-test and the one-way ANOVA, while those with skewed distribution and unequal variance were analyzed with nonparametric approaches (Mann-Whitney *U* test). Significant differences were considered at $P \leq 0.05$. Data were calculated as mean ± standard error (SE).

3. Results

3.1. Characterization of AgNPs and PSNPLs

The size-frequency distribution of AgNPs and PSNPLs was determined *via* representative TEM images, as shown in supplementary data (Fig. S1). The average diameter of AgNPs is <10 nm (7.2 ± 2.4), while plastic particles whether PS-50 or PS-500 have wider diameters (43.6 ± 12.2 and 415.0 ± 12.9, respectively). Further approaches were conducted to describe their morphology, degree of aggregation, and charge Fig. 1 (A-H). TEM images clearly showed differences in the morphology of PSNPLs alone (A and D) with those combined with AgNPs (B and E). AgNPs are observed stacked upon the outer border of the plastic nanospheres of PS-50

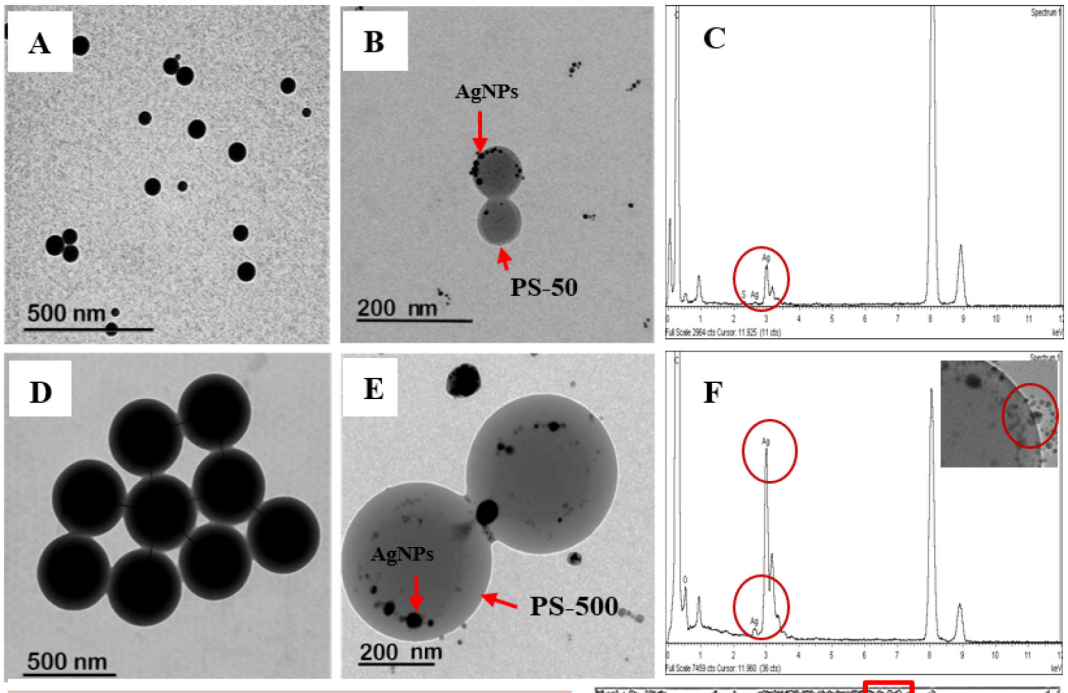

G	Hydrodynamic size (nm)	PDI	Zeta potential ζ (mV)
AgNPs	12.84±7.333	0.275±0.062	-30.3±2.84
PS-50+AgNPs	58.4±1.289	0.173±0.023	-51.8±1.29
PS-500+AgNPs	434.4±10.02	0.108±0.04	-54±0.351
PS-50	73.74 ± 1.88	0.053±0.006	-49.71 ± 0.66
PS-500	488.91 ± 8.62	0.083±0.022	-53.01 ± 1.99

Fig. 1. TEM image of PS-50 (A), AgNPs adsorbed upon PS-50 edge (B), Energy dispersive X-ray spectroscopy (EDX) of AgNPs + PS-50 (C). TEM image of PS-500 (D), AgNPs adsorbed upon PS-500 (E), Energy dispersive X-ray spectroscopy (EDX) of AgNPs + PS-500 (F). Hydrodynamic size and Zeta potential values (G). The FTIR spectra for PS-50 and PS-500 (H).

regularly like ring lobes (B), as well as with large size plastic particles in PS-500, but with low regular distribution (E). The silver nature was confirmed by EDX (C and F). The evaluated hydrodynamic size of AgNPs is very small (12.84 ± 7.33) in comparison with that of plastic particles (73.74 ± 1.88 and 488.91 ± 8.62) and agrees with their TEM sizes. Interestingly, the hydrodynamic size of plastic and silver combination (AgNPs + PS-50 and AgNPs + PS-500) is lower than PSNPLs alone (58.4 ± 1.29 and 434.4 ± 10.02), respectively (G). Both AgNPs and PSNPLs dispersions show high values of zeta potential indicating they are well dispersed. The negative charge of PSNPLs can be attributed to sulfate groups of potassium persulfate used in their synthesis. The FTIR spectra of both PS-50 and PS-500 agree with the expected for polystyrene (H). They show peaks around 3000 cm^{-1} indicative of CH_2 and a mono-substituted benzene ring, while saturated C—H of methylene stretches are below 3000 cm^{-1} and the unsaturated C—H from the benzene ring stretches fall above 3000 cm^{-1}. The other strong peaks are apparent around 1500 cm^{-1} confirming the benzene ring that typically falls from 1620 to 1400 cm^{-1}. Additionally, benzene fingers as a series of weak bands which fall from 1650 to 2000 cm^{-1} are related to the mono-substituted benzene ring of polystyrene.

3.2. Drosophila viability after exposures

Silver compounds, regardless of their form, and PSNPLs regardless of their size, whether administrated alone or in combination failed to induce significant decreases in *Drosophila* viability Fig. 2 (A and B). The experiment was carried out using five replicates of 250 eggs for each concentration scenario (0.2 mM and 1 mM) as well as for untreated medium, used as the negative control. It should be remembered that in Section 2.2 we have indicated the relationship between the concentrations expressed in mM, and the amount of μg of the different compounds per g of food medium. The adults were collected and counted to calculate the percentage of viability regarding the negative control. The emerged adults were investigated for any morphological changes. It is noticeable that the PSNPLs/silver coexposure reduced the faint pigmentation caused by silver exposure, especially at the higher tested scenario (1 mM). Generally, the treated/untreated adults emerged through two days, the eleventh and twelfth from seeding eggs. Interestingly, PSNPLs exposure, when coadministered with the silver compounds, improves adult emergence by reducing the delay induced by silver exposure Fig. 2 (C and D).

For the AgNPs (0.2 mM) experiment, cotreatments with PS-50 and PS-500 significantly reduce delay in adult emergence moving from 61 % of emerged adults on day 11th to 97 % and 94 %, respectively. Similarly, AgNPs (1 mM) induced a similar trend but with less effect moving from 65 % to 82 % and 76 %, respectively. Regarding $AgNO_3$ exposures, these effects are clearly observed at the concentration of 1 mM where the emergence of 7 % of adults at the eleventh is significantly enhanced to 46 % and 77 % after coexposure with PS-50 and PS-500, respectively.

3.3. Internalization of silver compounds and PSNPLs

3.3.1. Silver content detection in larval body by using ICP-MS

One open question is if PSNPLs can act as carriers of environmental pollutants, including metals, modulating their uptake. To such end, we have determined if silver concentrations inside *Drosophila* larvae differ when larvae are exposed to only AgNPs or $AgNO_3$, regarding their coexposures

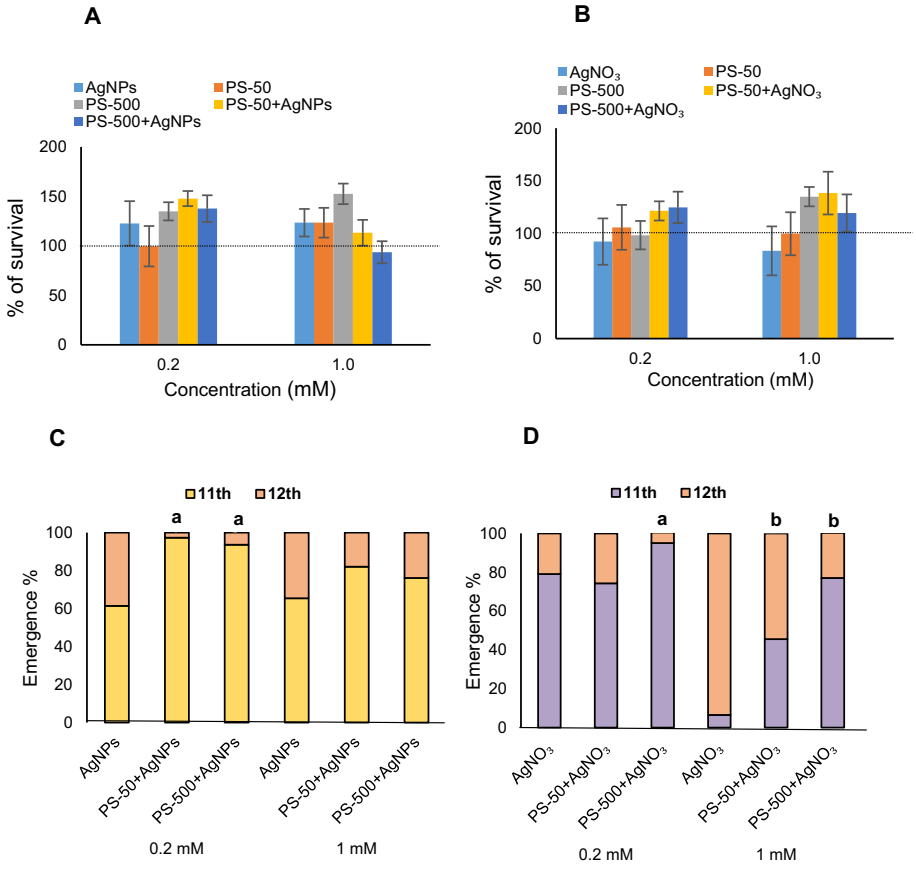

Fig. 2. Egg-to adult survival rate of *Drosophila* flies treated with AgNPs/$AgNO_3$, PSNPLs (PS50/PS500) and their combinations (A and B). Percentages of emergence (emergence at 11th day and 12th day) of *Drosophila* flies treated with AgNPs + PSNPLs (C) or $AgNO_3$ + PSNPLs (D), regarding those treated with AgNPs or $AgNO_3$, respectively. Statistically significant ($P \leq 0.05$), (a) *vs* (0.2 AgNPs/$AgNO_3$) and (b) *vs* (1 AgNPs/$AgNO_3$).

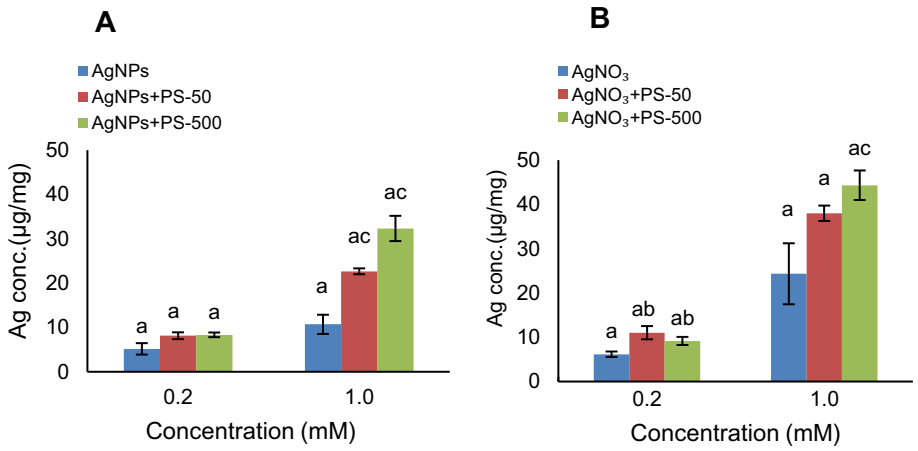

Fig. 3. Silver concentration inside *Drosophila* larvae tissues after exposure to AgNPs and AgNPs + PSNPLs (A) or to $AgNO_3$ and $AgNO_3$ + PSNPLs (B). Statistically significant ($P \leq 0.05$), (a) *vs* negative control (0.04 µg/mg), (b) *vs* (0.2 mM AgNPs/$AgNO_3$) and (c) *vs* (1 mM AgNPs/$AgNO_3$).

with PSNPLs. As indicated in Fig. 3 (A and B, respectively) the silver content of cotreated larvae is significantly higher than in the silver (AgNPs or $AgNO_3$) treatments alone. The effect is dose-dependent, reaching very significant effects at the higher dose (1 mM) of both silver compounds. At that dose, PSNPLs (PS-50 and PS-500) clearly magnified the levels of internalized silver when coexposed. Thus, the internal levels of silver after AgNPs (10.70 µg/mg) and $AgNO_3$ (24 µg/mg) exposures are increased in their coexposures with PS-50 (22.67 and 32.33 µg/mg) and PS-500 (38 and 44 µg/mg), respectively. It is interesting to point out that these effects are more marked when the coexposure involves the large size of PSNPLs (PS-500).

3.3.2. PSNPLs/silver internalization detection by using TEM

TEM was used to monitor the internalization of PSNPLs (PS-50 and PS-500) alone or in combination with AgNPs. To get a better description of the uptake process, the different stages of the journey of PSNPLs through the ingestion route were described by using TEM images. The different evaluated stages comprise their interaction with midgut lumen components, their interaction with the enterocytes constituting the intestinal barrier, and the interaction with hemocoel cavity components (including hemocytes) once PSNPLs cross the intestinal barriers (Figs. 4, 5, and 6, respectively).

3.3.2.1. PSNPLs (PS-50 and PS-500) internalization. Fig. 4 describes the internalization of PS-50 (A, B, and C) and PS-500 (D, E, and F) inside the *Drosophila* larvae body. Both plastic particles PS-50 and PS-500 were observed distributed inside the midgut lumen (A and D), before penetrating the peritrophic membrane to reach intestinal enterocyte cells (B and E) and, finally, reached the hemocoel compartment once translocated through the intestinal barrier (C and F). It is interesting to note that PS-50 are distributed in *Drosophila* larval midgut lumen in batches showing aggregation (A) while PS-500 are found to be individually distributed (D). The

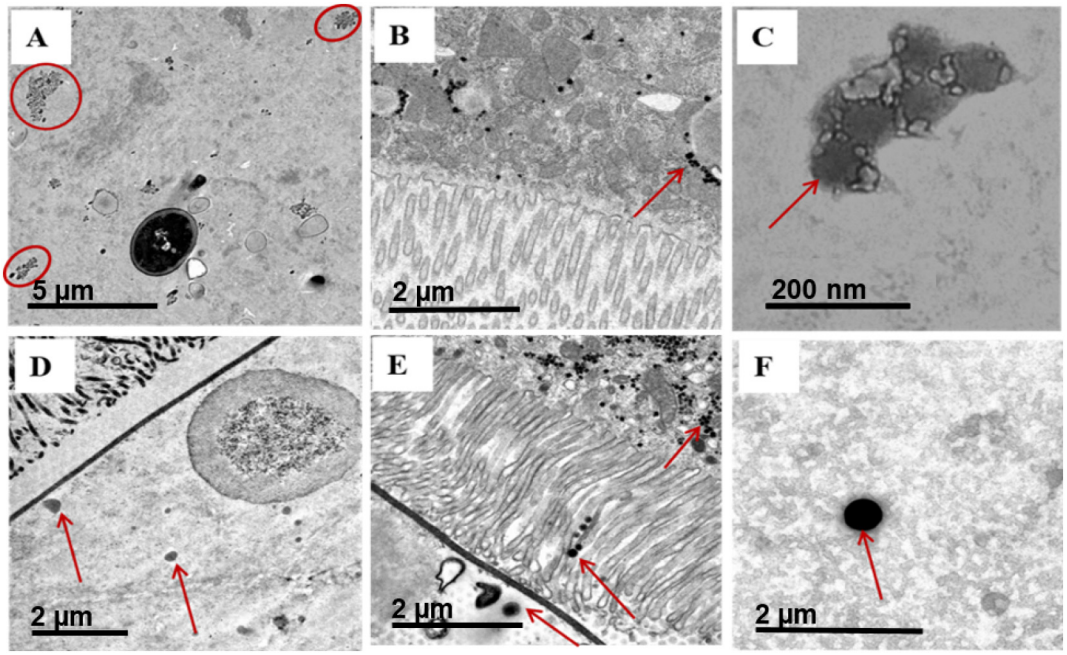

Fig. 4. TEM images of PS-50 (A, B, and C) and PS-500 (D, E, and F) internalization in *Drosophila* larvae. In the midgut lumen (A and D), inside the cytoplasm of midgut enterocytes (B and E) and in the hemolymph (C and F).

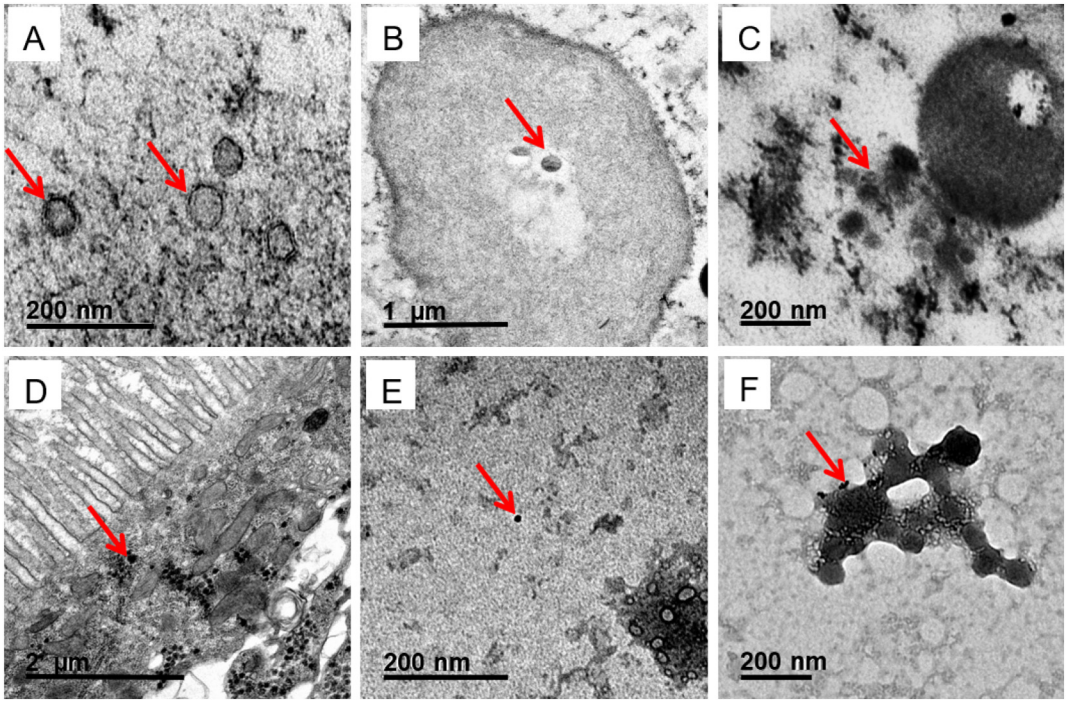

Fig. 5. TEM images of AgNPs + PS-50 internalization through Drosophila' larvae. Distributed inside midgut lumen (A), inside or surrounding microbiota of midgut lumen (B and C) or inside cytoplasm of midgut enterocytes (D). AgNPs whether located individually (E) or attached to PS-50 (F) in hemolymph of treated larvae.

success of PSNPLs to be internalized inside the larval tissue could facilitate their mission of acting as a potential carrier facilitating silver particles to internalize.

3.3.2.2. PS-50/AgNPs internalization. TEM is also a useful tool to follow up on the internalization of AgNPs + PS-50 at different biological stages as indicated in Fig. 5. Complexes are observed inside the midgut lumen (A), where AgNPs were clearly observed at the outer surface of PS-50 particles that are distributed inside the midgut lumen. AgNPs + PS-50 also appear inside (or surrounding) the microbiota of the midgut lumen (B and C) or distributed in the cytoplasm of midgut enterocytes (D). The investigation of hemolymph samples of treated larvae with AgNPs/PS-50 showed the

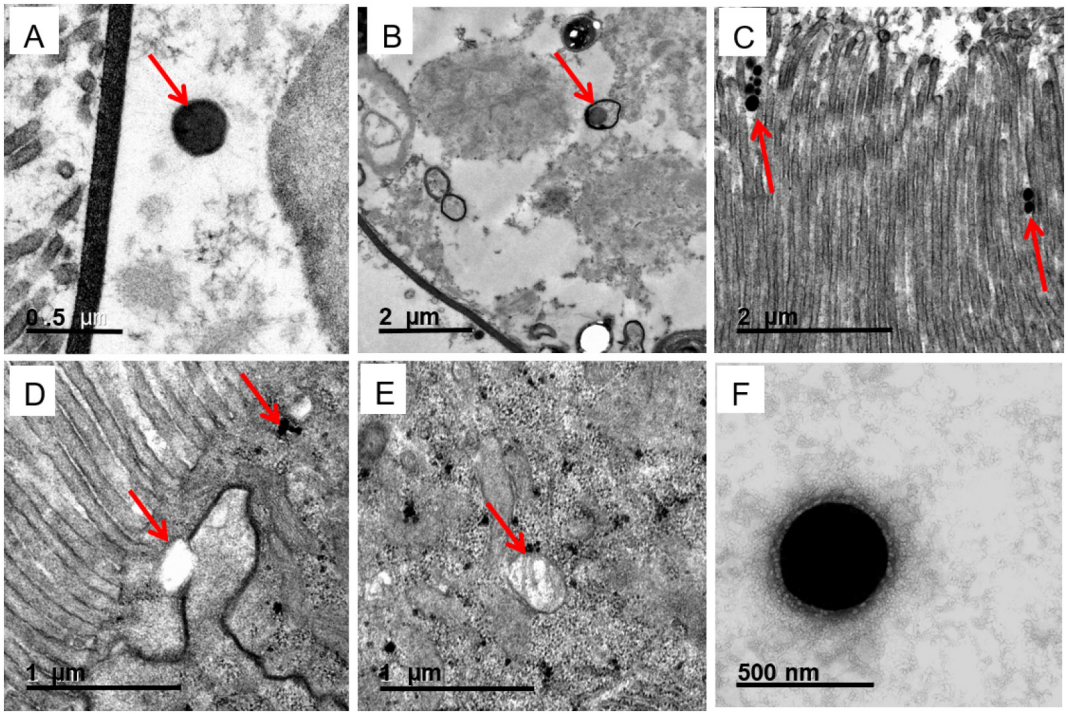

Fig. 6. TEM images of AgNPs + PS-500 internalization through Drosophila' larvae. The complex is distributed inside the midgut lumen near to peritrophic membrane (A), surrounded completely by intestinal vacuole (B) moving among enterocytes' microvilli (C), inside cytoplasm of midgut enterocytes, and penetrating cells borders (D), damaging cellular mitochondria (E) and, finally, reaching the hemolymph (F).

presence of Ag nanoparticles whether located individually (E) or attached to PS-50 (F).

3.3.2.3. PS-500/AgNPs internalization. The large size of PS-500 facilitates their detection through the ingestion process. Thus, TEM images of AgNPs + PS-500 through their journey until their internalization in the larvae body are presented in Fig. 6. Thus, PS-500 as large spherical particles are observed inside the midgut lumen near to peritrophic membrane of the larvae intestine (A). In this case, AgNPs are not clearly observed due to the high contrast of plastic particles with their black color. Inside the lumen, PS-500/AgNPs complexes were surrounded completely by intestinal vacuoles (B) before penetrating the peritrophic membrane to move among enterocytes' microvilli (C). The existence of these large plastic particles in the cytoplasm of the intestinal cells, and due to their kinetics energy, mediate harmful impacts appearing as holes in the cell borders (D) and in the mitochondria (E). Finally, the PS-500 journey overcomes the intestinal barrier, translocating and reaching the hemolymph (F).

3.4. Gene expression changes

One of the major aims of this study is to unveil the *in vivo* molecular responses to the coexposure of plastic particles with heavy metals. Accordingly, we have evaluated changes in the expression levels of genes involved in different pathways/mechanisms, and the obtained results are presented in Fig. 7. As observed, the heat-shock protein gene (*Hsp70)* showed deregulation after the exposure to AgNPs/$AgNO_3$ or PSNPLs alone or administered as a combination. It must be indicated that the highest expression level was associated with the exposure to the highest $AgNO_3$ dose (1 mM), which is reflected in the high expression levels observed in its coexposure with PSNPLs. Similarly, the *Hsp83* gene also showed deregulation but milder, and this expression was not affected by the applied dose of AgNPs/$AgNO_3$. To address the antioxidant response at the molecular level, the expression of *Sod2* and *Cat,* as reliable genes, was examined. Although there is an opposite effect between AgNPs/$AgNO_3$ and PSNPLs regarding the expression of *Sod2,* their coexposure returned its expression to the basal level. The expression levels of *Cat* were low in AgNPs, PSNPLs, or in the coexposure experiments. It is important to point out that the coexposure reduced the *Cat* expression levels produced by the exposure to the highest dose of AgNPs (1 mM). Regarding the effects of the *Cat* expression levels after the $AgNO_3$ exposures, they were significantly increased at the highest dose, in contrast with the low levels observed with the PSNPLs exposure. Interestingly, the coexposure (PSNPLs + $AgNO_3$) mediated a significant up-regulation of the *Cat* expression levels, independently of the PSNPLs size. It is notorious the induced de-regulation of the intestinal physical stress genes (*Duox* and *PPO2*) after exposure to PSNPLs, mainly at the higher size (PS-500) for *PPO2*. This downregulation was partially recovered in the combination with silver compounds mainly for *Duox*. All this would point out that the physical stress induced in the intestinal barrier by PSNPLs is partially recovered when combined with silver compounds. Genotoxicity, and especially oxidative DNA damage, is an important target to evaluate

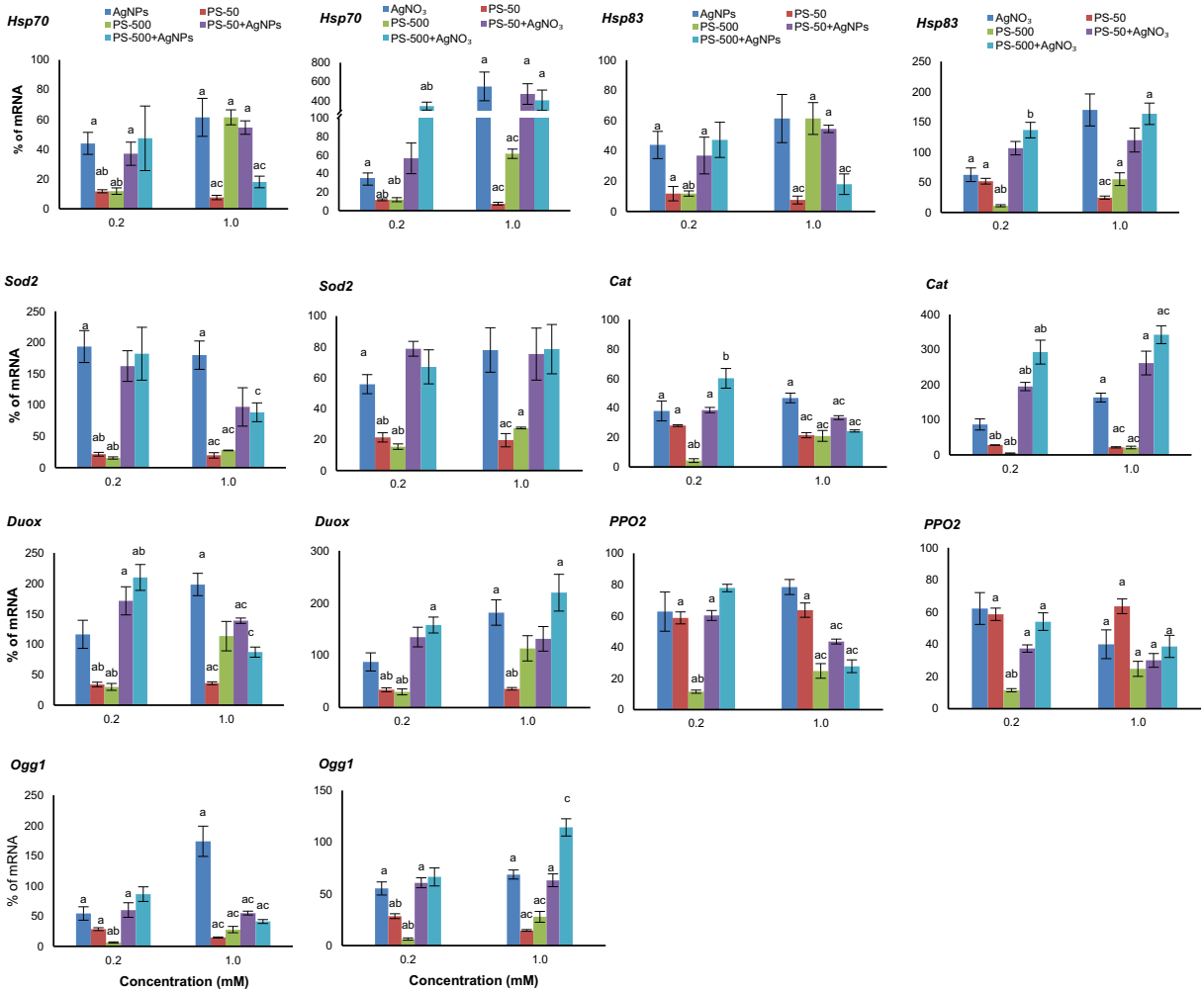

Fig. 7. Gene expression levels in Drosophila' larvae after exposure to AgNPs, PSNPLs and AgNPs + PSNPLs or to $AgNO_3$, PSNPLs and $AgNO_3$ + PSNPLs. General stress genes (*Hsp70* and *Hsp83*), antioxidant genes (*Sod2* and *Cat*), intestinal physical stress genes (*Duox* and *PPO2*), and DNA repair gene (*Ogg1*). Statistically significant ($P \leq 0.05$), (a) *vs* negative control, (b) *vs* (0.2 mM AgNPs/$AgNO_3$) and (c) *vs* (1 mM AgNPs/$AgNO_3$). The lack of a letter in a column indicates no statistical differences.

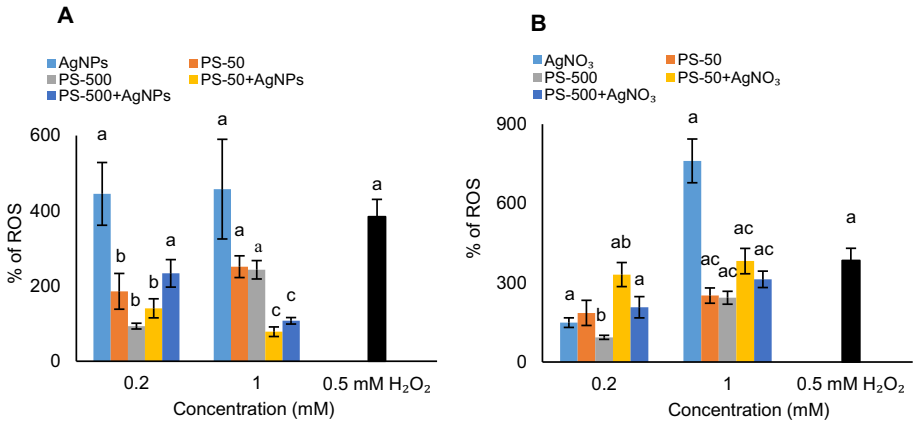

Fig. 8. Oxidative stress induced in hemocytes of *Drosophila* larvae exposed to AgNPs, PSNPLs and AgNPs + PSNPLs (A) or $AgNO_3$, PSNPLs and $AgNO_3$ + PSNPLs (B). Statistically significant ($P \leq 0.05$), (a) *vs* negative control, (b) *vs* (0.2 mM AgNPs/$AgNO_3$) and (c) *vs* (1 mM AgNPs/$AgNO_3$). The lack of a letter in a column indicates no statistical differences.

the harmful effects of exposures. Herein the expression of *Ogg1* was investigated after silver and plastic particles exposure. It is noticeable that the up-regulation of the *Ogg1* gene after the exposure to 1 mM of AgNPs was reduced in the coexposure with PSNPLs at the same dose. Similarly, the PSNPLs coexposure with $AgNO_3$ at the highest dose (1 mM) reduced the effects induced by $AgNO_3$ alone.

3.5. Oxidative stress induction

Oxidative stress induction has been extensively proposed as the main factor standing behind the detrimental impact of nanomaterials. Herein, silver compounds exposures produced a significant elevation of the oxidative stress levels in the hemocytes of the exposed larvae, in comparison with untreated ones and in all studied exposure scenarios (Fig. 8). Although PSNPLs were able to induce some oxidative stress at the high dose (1 mM), this effect could not be detected at the low concentration scenario (0.2 mM). Importantly, when the oxidative stress levels induced by the combinations AgNPs/$AgNO_3$ + PSNPLs are compared with those induced by AgNPs/$AgNO_3$ alone a significant reduction is observed confirming their antagonistic effects. These decreases are observed in all the cases with the exception of the $AgNO_3$ exposure in the low exposure scenario. Interestingly, both PS-50 and PS-500 show similar behavior in the coexposure scenario.

3.6. Genotoxic impact evaluated in the comet assay

The genotoxicity of silver (AgNPs/$AgNO_3$), PSNPLs (PS-50 and PS-500), and their coexposures were determined using the comet assay as a tool to detect DNA strand-breaks induction. The obtained results are indicated in Fig. 9, and DNA damage induction was determined as the percentage of DNA present in the tail section of the comet images. From these results, several points need to be highlighted. The first point is that both silver compounds induced significant increases in the levels of DNA breaks, $AgNO_3$ inducing more damage mainly at the highest concentration. The second point is that both PSNPL sizes (PS-50 and PS500) also induced significant increases in the levels of DNA damage, PS-50 being more genotoxic than PS-500. Third, and more relevant, the combination of both PSNPLs with the two selected silver compounds significantly reduced its potential DNA damaging effects. These results are very representative of the antagonistic relationship established when both sets of compounds are evaluated.

4. Discussion

The behavior of MNPLs in the different environmental compartments is considered an emerging topic, mainly due to their ability to absorb certain hazardous pollutants (including heavy metals) sharing the same

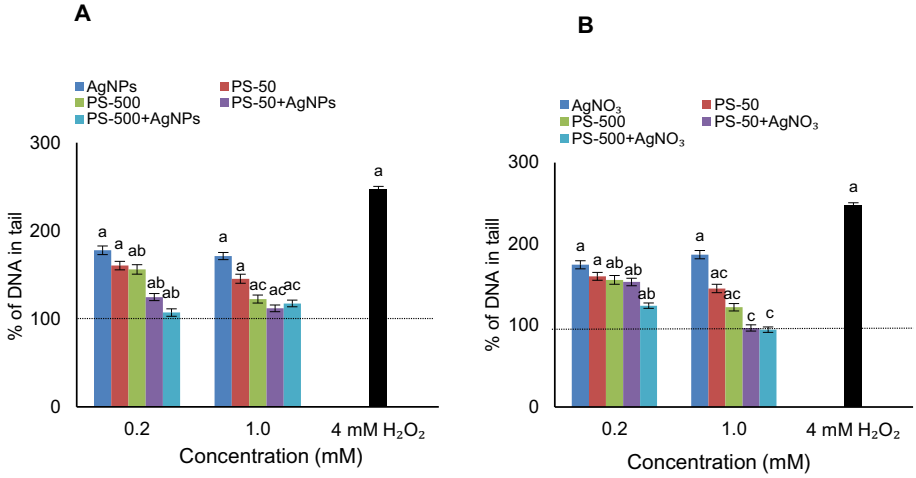

Fig. 9. DNA damage levels in *Drosophila* larvae hemocytes after exposure to AgNPs, PSNPLs, and AgNPs + PSNPLs (A) or $AgNO_3$, PSNPLs, and $AgNO_3$ + PSNPLs (B). Statistically significant ($P \leq 0.05$), (a) *vs* negative control, (b) *vs* (0.2 mM AgNPs/$AgNO_3$) and (c) *vs* (1 mM AgNPs/$AgNO_3$).

environments (Zhou et al., 2022). Such absorption capacities can significantly modulate the potential impacts of such pollutants, by changing their physicochemical properties (Bhagat et al., 2021). Nonetheless, there is limited information regarding the hazardous scenario resulting from the MNPLs/pollutants combinations, and the potential mechanisms involved in such types of interactions (Cao et al., 2021). In our case, the physicochemical properties of PSNPLs indicate that both plastic sizes (PS-50 and PS-500) are well dispersed and with a negative charge similar to that of AgNPs. The interaction of PSNPLs and AgNPs was confirmed morphologically by TEM images, and chemically through TEM-EDX analysis. Fortunately, the smaller size of silver nanoparticles (7 nm) revealed how they can be sorted regularly stack upon the outer border of the spherical particles of PSNPLs, especially for the smaller ones (PS-50). In addition, the TEM images picked up by the high TEM resolution showed the ability of silver particles to infiltrate inside PSNPLs, especially for the larger ones (PS-500), presumable by forming sandwiched π-stacking structures with the side benzene rings of polystyrene (Feng et al., 2022).

At present, there are many questions regarding the potentially harmful impacts of nanoplastics exposure. It is necessary to know if such effects are related to its polymer structure (physical stress) or owing to the adsorption of various pollutants (chemical stress). In addition, we need to know if the behavior of the combination MNPLs-pollutants is synergistic or antagonistic and if such interactions are size- or dose-dependent. All of these questions drive our work and are discussed in the current study. Firstly, it is interesting to point out that the survival rates were not affected whether *Drosophila* larvae were exposed to silver compounds (AgNPs/$AgNO_3$) or PSNPLs (PS-50/PS-500) administrated each alone or together, at doses up to 1 mM. A recent *in vitro* study using human intestinal Caco-2 cells, showed that exposures to AgNPs/$AgNO_3$ alone or in combination with PSNPLs reduced cell viability, although PSNPLs alone failed to induce any toxic impacts at all studied doses (Domenech et al., 2021). Contrarily, herein we have observed that coexposures were able to restore the reduced pigmentation of emerged *Drosophila* adults induced by silver, especially after $AgNO_3$ exposures. Moreover, PSNPLs when coadministered with silver decrease the emergence delay resulting from exposure to silver alone regardless of its form. These effects are the first indication of an antagonistic interaction between silver and MNPLs. This behavior has also been recently reported by Zhang et al. who found that PSMPLs exposure reduces the toxic effects of silver in *Escherichia coli*, *Selenastrum capricornutum*, *Daphnia magna,* and zebrafish. The authors attributed this behavior to the attachment of MPLs capacity, which could modify silver chemical speciation (Zhang et al., 2021). The reduced toxicity of the complexes' PSNPLs/micropollutants might be attributed to the reduced bioavailability of the adsorbed micropollutants (Verdú et al., 2022). This sorption ability does not reduce the ability of silver to be incorporated into the organisms as observed using ICP-MS, where PSNPLs significantly increased the presence of silver in *Drosophila* larvae tissues, especially under the high dose (1 mM) scenario. This would support the proposal that nanoplastics can act as heavy metal vectors (Maity et al., 2021). Interestingly, this increase in the internalization inside the body tissue is mainly observed after the cotreatment with PS-500. This means that PS-500 can transfer more silver (regardless of its form) into *Drosophila* tissues rather than PS-50. This disagrees with the proposal that heavy metals' adsorption is increased as the surface of plastic particles increases (Guo et al., 2020). At this point, it must be pointed out that while PS-50 are observed in aggregated batches PS-500 are distributed individually, showing some roughness when present inside the midgut lumen of *Drosophila* larvae. Thus, our findings would agree with the proposal that there are positive correlations between roughness and heavy metal adsorption (Qi et al., 2021). It is important to indicate that the pH changes occurring inside the *Drosophila* midgut (Overend et al., 2016) might affect large plastic particles more than smaller ones. The pH conditions can control the adsorption capacity of plastic particles to heavy metals by deprotonating functional groups on the nanoplastics surface, increasing the electronegativity and adsorption sites that facilitate the adsorption of heavy metals (Lin et al., 2021).

Despite the importance of tracking the internalization of nanoplastics materials and their sorbent pollutants, the available data at present remain insufficient, especially at the *in vivo* level (Paul et al., 2020). Accordingly, we wish to emphasize the interest of our work using TEM methodology as an essential tool to follow up the complete journey of the complexes' PSNPLs/Ag-compounds from the larvae mouth, to their interactions with gut components, their interaction with the intestinal barrier, their translocation through the barrier to reach hemolymph (as homologous of blood), and interacting with hemocytes (as homologous of lymphocytes). Interestingly, nanoplastics followed the same journey pattern as observed for different nanomaterials (Alaraby et al., 2018, 2021). The use of hemocytes as a target is relevant, not only because of the functionality of such cells but because indicating that the complexes are able to cross the intestinal barrier and spread by organs and tissues. Thus, MNPLs associated with benzo(*a*)pyrene were observed to affect mussel hemocytes indicating their ability to cross the intestinal barrier (Katsumiti et al., 2021). Although PSNPLs, regardless of their size, are able to internalize into the intestinal, as also demonstrated in zebrafish (Sendra et al., 2021), the internalization pathways would depend on their size. Thus, while small particles PS-50 uptake mainly *via* clathrin- and caveolae-mediated pathways, PS-500 would uptake *via* macropinocytosis (Liu et al., 2021a). In our case, PS-500 were observed surrounded completely by vacuoles, pointing out a potential role of midgut vacuoles in the PSNPLs uptake/translocation in *Drosophila* larvae (Alaraby et al., 2021). The internalization of PS-500 inside the enterocytes of *Drosophila* larvae was associated with damaged cell borders, as well as damaged mitochondria, which was also observed in human intestinal Caco-2 cells (Xu et al., 2021). All of this would be indicative of the physical stress induced by MNPLs exposure.

To address the physical stress induced by MNPLs as well as the chemical stress attributed to the attached silver compounds, changes in the expression levels of a wide battery of genes were investigated. This approach is useful for the detection of mild effects. Thus, the expression levels of the highly conserved stress genes *Hsp70* and *Hsp83* were altered after silver exposures in comparison with PSNPLs exposure. Nevertheless, no relevant changes were observed in the coexposures, regarding those induced by silver compounds alone. The negative impact of silver (regardless of its form) on the expression of the *Hsp* genes in *Drosophila* has already been reported, in particular for *Hsp70* (Ahamed et al., 2010; Alaraby et al., 2019). The expression of the antioxidant genes *Sod2* and *Cat* were greatly down-regulated with exposure to PSNPLs alone, which could be attributed to the oxidative stress produced by PSNPLs exposure (Liu et al., 2020; Li et al., 2020a). Regarding the effects of coexposures, is relevant to point out the increased expression levels observed for *Cat* after the high exposure scenario with $AgNO_3$. In such conditions, the effects induced by the cotreatment were significantly higher than those induced by the silver compound. These results would point to an interaction effect of the coexposure. The expression levels of the genes *Duox* and *PPO2*, as responding to the induction of intestinal physical stress, have shown to be sensitive to any stress introduced by nano-scaled materials upon the intestinal barrier (Alaraby et al., 2016b, 2020). In our study, they were de-regulated with exposures to silver or PSNPLs, indicating their interaction with the intestinal barrier as confirmed by the TEM and ICP-MS results. Regarding the effects of coexposures, interactions were observed for *Duox* under coexposures with AgNPs at the low exposure scenario, with higher expression levels than those observed for AgNPs alone. Regarding the *PPO2* gene, the interactions were observed under the high exposure scenario but, in this case, the coexposures induced expression levels than the AgNPs alone. Altogether, these data confirm the differential effects induced by the coexposures. Finally, changes in the expression levels of the *Ogg1* gene were determined, as a potential response to oxidative stress damaging DNA. From the set of obtained data, we can point out those observed after AgNPs exposure under the highest concentration scenario. In such conditions, the coexposures reduced significantly the expression levels induced by AgNPs alone. Interestingly, this observed effect match well with the data obtained in the detection of the intracellular levels of ROS.

The induction of oxidative stress is considered one of the mechanisms involved in the hazardous effects of nanomaterials (Mendoza and Brown, 2019). In our study, the exposure to both silver and PSNPLs mediated oxidative stress induction, but to different degrees. It has been reported that silver compounds, independently of their form, induced oxidative stress in different organisms including *Drosophila* (Alaraby et al., 2019; Singh et al., 2021), while for MNPLs these effects have been recently reviewed (Kumar et al., 2022). It is important to note that cotreatments succeeded to diminish the oxidative stress induced by silver, especially by AgNPs, independently of the exposure scenario. This also occurs after $AgNO_3$ exposure, but only under the high exposure scenario. All this confirms the antagonistic effects of coexposures. Although Bhagat et al. (2021) in their review found more than ten studies pointing out the antagonistic interaction of MNPLs with other pollutants, our study is the first one showing the effects on oxidative stress levels.

There is a strong link between oxidative stress and genotoxicity; thus, any disturbance in the redox balance can mediate a genotoxic impact (AshaRani et al., 2009; Dutta et al., 2018). In our study, silver compounds (regardless of their form) caused pronounced DNA damage levels in the hemocytes of *Drosophila* larvae. This is something well-known in many organisms, including *Drosophila* (Alaraby et al., 2019). More interesting are the results showing that PSNPLs (regardless of their form) also act as genotoxic agents. Only a very recent paper reported the genotoxic effects of PSMPLs in *Drosophila* but it used the wing-spot assay, which measures the induction of somatic mutation or somatic recombination, and microplastics measuring between 4 and 20 μm (Demir, 2021). Nevertheless, MNPLs induced genotoxic damage in different human hematopoietic cells (Rubio et al., 2020), as well as in mussel hemocytes (Gonçalves et al., 2022). But no studies on the cotreatment effects have been addressed until now. Herein, coexposure of PSNPLs (bot sizes) with silver compounds ($AgNPs/AgNO_3$) significantly reduced the DNA damage induced by silver compounds alone. It is important to note that the properties of nanoplastics enhancing or mitigating the action of heavy metals are still unclear (Huang et al., 2021). For instance, the interaction of heavy metals and nanoplastics might be antagonistic or synergistic according to the concentration (Li et al., 2020b) or the pH (Lin et al., 2021). Nevertheless, the antagonistic action of PSNPLs observed in the current study was observed independently of the PSNPLs' size and the exposure scenario. Such interaction might be owing to their ability to confine silver ions or silver nanoparticles and, therefore, reduce their bioavailability and, consequently, their potentially harmful impacts. Moreover, heavy metals, whether in ion forms or as nanoparticles can infiltrate or enter the pores of the nanoplastic particles (Liu et al., 2021b) which could reduce their activity.

5. Conclusions

The interaction of heavy metals with plastics specks is a potential parameter that could modulate their potentially harmful impacts. This is a relevant topic due to the coexistence of both types of environmental pollutants in common environmental compartments. Our results, as a whole, provide data pointing out an antagonistic interaction between them. Thus, nanoplastics have successes as metal carriers, cooperating in transferring silver compounds into deep tissues and hemolymph at rates exceeding the observed levels after silver exposure alone. The molecular response of a set of genes modulating different functional pathways affect differentially coexposures than single exposures. Furthermore, the oxidative stress and genotoxicity mediated by silver compounds were reduced when coexposures were applied. Consequently, our data confirms an antagonistic interaction between PSNPLs and silver compounds (regardless of their form) ameliorating the harmful effects associated with silver exposures. The relevance of the reported data suggests carrying out further systematic studies aiming to add new data to better understand the mechanism of interaction between nanoplastic and heavy metals.

Supplementary data to this article can be found online at https://doi.org/10.1016/j.scitotenv.2022.156923.

CRediT authorship contribution statement

RM and AH planned the experiments. MA, DA and AV carried out the experimental part. MA and DA analyzed the data, carried out the statistical analysis, and prepared tables/figures. MA, DA, RM, and AH wrote the final manuscript.

Declaration of competing interest

The authors declare they have no actual or potential competing financial interests.

Acknowledgments

This project has received funding from the European Union's Horizon 2020 research and innovation program under grant agreement No 965196 (PlasticHeal). This work was partially supported by the Spanish Ministry of Science and Innovation [PID2020-116789, RB-C43].

M. Alaraby held a postdoctoral fellowship from the Cultural Affairs Sector and Missions (Ministry of Higher Education), Egypt.

A. Villacorta was supported by a PhD fellowship from the National Agency for Research and Development (ANID), CONICYT PFCHA/DOCTORADO BECAS CHILE /2020-72210237.

References

Ahamed, M., Posgai, R., Gorey, T.J., Nielsen, M., Hussain, S.M., Rowe, J.J., 2010. Silver nanoparticles induced heat shock protein 70, oxidative stress and apoptosis in drosophila melanogaster. Toxicol. Appl. Pharmacol. 242 (3), 263–269. https://doi.org/10.1016/j.taap.2009.10.016.

Alaraby, M., Annangi, B., Hernández, A., Creus, A., Marcos, R., 2015. A comprehensive study of the harmful effects of ZnO nanoparticles using *Drosophila melanogaster* as an *in vivo* model. J. Hazard. Mater. 296, 166–174. https://doi.org/10.1016/j.jhazmat.2015.04.053.

Alaraby, M., Annangi, B., Marcos, R., Hernández, A., 2016a. Drosophila melanogaster as a suitable in vivo model to determine potential side effects of nanomaterials: a review. J. Toxicol. Environ. Health Part B 19, 65–104. https://doi.org/10.1080/10937404.2016.1166466.

Alaraby, M., Hernández, A., Marcos, R., 2016b. New insights in the acute toxic/genotoxic effects of CuO nanoparticles in the in vivo drosophila model. Nanotoxicology 10 (6), 749–760. https://doi.org/10.3109/17435390.2015.1121413.

Alaraby, M., Hernández, A., Marcos, R., 2018. Systematic in vivo study of NiO nanowires and nanospheres: biodegradation, uptake and biological impacts. Nanotoxicology 12 (9), 1027–1044. https://doi.org/10.1080/17435390.2018.1513091.

Alaraby, M., Romero, S., Hernández, A., Marcos, R., 2019. Toxic and genotoxic effects of silver nanoparticles in drosophila. Environ. Mol. Mutagen. 60 (3), 277–285. https://doi.org/10.1002/em.22262.

Alaraby, M., Demir, E., Domenech, J., Velázquez, A., Hernández, A., Marcos, R., 2020. In vivo evaluation of the toxic and genotoxic effects of exposure to cobalt nanoparticles using Drosophila melanogaster. Environ. Sci. Nano 7 (2), 610–622. https://doi.org/10.1039/C9EN00690G.

Alaraby, M., Hernández, A., Marcos, R., 2021. Novel insights into biodegradation, interaction, internalization and impacts of high-aspect-ratio TiO2 nanomaterials: a systematic in vivo study using Drosophila melanogaster. J. Hazard. Mater. 409, 124474. https://doi.org/10.1016/j.jhazmat.2020.124474.

Alaraby, M., Abass, D., Domenech, J., Hernández, A., Marcos, R., 2022. Hazard assessment of ingested polystyrene nanoplastics in drosophila larvae. Environ. Sci.: Nano 9, 1845–1857. https://doi.org/10.1039/D1EN01199E.

Amelia, T.S.M., Khalik, W.M.A.W.M., Ong, M.C., Shao, Y.T., Pan, H.J., Bhubalan, K., 2021. Marine microplastics as vectors of major ocean pollutants and its hazards to the marine ecosystem and humans. Prog. Earth Planet. Sci. 8 (1), 1–26. https://doi.org/10.1186/s40645-020-00405-4.

AshaRani, P.V., Low Kah Mun, G., Hande, M.P., Valiyaveettil, S., 2009. Cytotoxicity and genotoxicity of silver nanoparticles in human cells. ACS Nano 3 (2), 279–290. https://doi.org/10.1021/nn800596w.

Bhagat, J., Nishimura, N., Shimada, Y., 2021. Toxicological interactions of microplastics/nanoplastics and environmental contaminants: current knowledge and future perspectives. J. Hazard. Mater. 405, 123913. https://doi.org/10.1016/j.jhazmat.2020.123913.

Cao, Y., Zhao, M., Ma, X., Song, Y., Zuo, S., Li, H., Deng, W., 2021. A critical review on the interactions of microplastics with heavy metals: mechanism and their combined effect on organisms and humans. Sci. Total Environ. 788, 147620. https://doi.org/10.1016/j.scitotenv.2021.147620.

Demir, E., 2021. Adverse biological effects of ingested polystyrene microplastics using Drosophila melanogaster as a model in vivo organism. J. Toxicol. Environ. Health A 84 (16), 649–660. https://doi.org/10.1080/15287394.2021.1913684.

Domenech, J., Cortés, C., Vela, L., Marcos, R., Hernández, A., 2021. Polystyrene nanoplastics as carriers of metals. Interactions of polystyrene nanoparticles with silver nanoparticles and silver nitrate, and their effects on human intestinal caco-2 cells. Biomolecules 11 (6), 859. https://doi.org/10.3390/biom11060859.

Dutta, S., Mitra, M., Agarwal, P., Mahapatra, K., De, S., Sett, U., Roy, S., 2018. Oxidative and genotoxic damages in plants in response to heavy metal stress and maintenance of genome stability. Plant Signal. Behav. 13 (8), e1460048. https://doi.org/10.1080/15592324.2018.1460048.

Fajardo, C., Martín, C., Costa, G., Sánchez-Fortún, S., Rodríguez, C., de Lucas Burneo, J.J., Nande, M., Mengs, G., Martín, M., 2022. Assessing the role of polyethylene microplastics as a vector for organic pollutants in soil: ecotoxicological and molecular approaches. Chemosphere 288, 132460. https://doi.org/10.1016/j.chemosphere.2021.132460.

Feng, H., Liu, Y., Xu, Y., Li, S., Liu, X., Dai, Y., Zhao, J., Yue, T., 2022. Benzo [a] pyrene and heavy metal ion adsorption on nanoplastics regulated by humic acid: cooperation/competition mechanisms revealed by molecular dynamics simulations. J. Hazard. Mater. 424, 127431. https://doi.org/10.1016/j.jhazmat.2021.127431.

Gigault, J., El Hadri, H., Nguyen, B., Grassl, B., Rowenczyk, L., Tufenkji, N., Feng, S., Wiesner, M., 2021. Nanoplastics are neither microplastics nor engineered nanoparticles. Nat. Nanotechnol. 16 (5), 501–507. https://doi.org/10.1038/s41565-021-00886-4.

Gonçalves, J.M., Sousa, V.S., Teixeira, M.R., Bebianno, M.J., 2022. Chronic toxicity of polystyrene nanoparticles in the marine mussel Mytilus galloprovincialis. Chemosphere 287, 132356. https://doi.org/10.1016/j.chemosphere.2021.132356.

Guo, X., Hu, G., Fan, X., Jia, H., 2020. Sorption properties of cadmium on microplastics: the common practice experiment and a two-dimensional correlation spectroscopic study. Ecotoxicol. Environ. Saf. 190, 110118. https://doi.org/10.1016/j.ecoenv.2019.110118.

Hansjosten, I., Takamiya, M., Rapp, J., Reiner, L., Fritsch-Decker, S., Mattern, D., Andraschko, S., Anders, C., Pace, G., Dickmeis, T., Peravali, R., 2022. Surface functionalisation-dependent adverse effects of metal nanoparticles and nanoplastics in zebrafish embryos. Environ. Sci.: Nano 9, 375–392. https://doi.org/10.1039/D1EN00299F.

Huang, W., Song, B., Liang, J., Niu, Q., Zeng, G., Shen, M., Deng, J., Luo, Y., Wen, X., Zhang, Y., 2021. Microplastics and associated contaminants in the aquatic environment: a review on their ecotoxicological effects, trophic transfer, and potential impacts to human health. J. Hazard. Mater. 405, 124187. https://doi.org/10.1016/j.jhazmat.2020.124187.

Katsumiti, A., Losada-Carrillo, M.P., Barros, M., Cajaraville, M.P., 2021. Polystyrene nanoplastics and microplastics can act as trojan horse carriers of benzo (a) pyrene to mussel hemocytes in vitro. Sci. Rep. 11 (1), 1–17. https://doi.org/10.1038/s41598-021-01938-4.

Khalid, N., Aqeel, M., Noman, A., Khan, S.M., Akhter, N., 2021. Interactions and effects of microplastics with heavy metals in aquatic and terrestrial environments. Environ. Pollut. 290, 118104. https://doi.org/10.1016/j.envpol.2021.118104.

Kumar, R., Manna, C., Padha, S., Verma, A., Sharma, P., Dhar, A., Ghosh, A., Bhattacharya, P., 2022. micro(nano)plastics pollution and human health: how plastics can induce carcinogenesis to humans? Chemosphere 298, 134267. https://doi.org/10.1016/j.chemosphere.2022.134267.

Lee, W.S., Cho, H.J., Kim, E., Huh, Y.H., Kim, H.J., Kim, B., Kang, T., Lee, J.S., Jeong, J., 2019. Bioaccumulation of polystyrene nanoplastics and their effect on the toxicity of au ions in zebrafish embryos. Nanoscale 11 (7), 3173–3185. https://doi.org/10.1039/c8nr09321k.

Li, Y., Liu, Z., Li, M., Jiang, Q., Wu, D., Huang, Y., Jiao, Y., Zhang, M., Zhao, Y., 2020a. Effects of nanoplastics on antioxidant and immune enzyme activities and related gene expression in juvenile Macrobrachium nipponense. J. Hazard. Mater. 398, 122990. https://doi.org/10.1016/j.jhazmat.2020.122990.

Li, Z., Yi, X., Zhou, H., Chi, T., Li, W., Yang, K., 2020b. Combined effect of polystyrene microplastics and dibutyl phthalate on the microalgae Chlorella pyrenoidosa. Environ. Pollut. 257, 113604. https://doi.org/10.1016/j.envpol.2019.113604.

Lin, Z.K.L., Hu, Y.W., Yuan, Y.J., Hu, B.W., Wang, B.L., 2021. Comparative analysis of kinetics and mechanisms for pb (II) sorption onto three kinds of microplastics. Ecotoxicol. Environ. Saf. 208, 111451. https://doi.org/10.1016/j.ecoenv.2020.111451.

Liu, Z., Huang, Y., Jiao, Y., Chen, Q., Wu, D., Yu, P., Li, Y., Cai, M., Zhao, Y., 2020. Polystyrene nanoplastic induces ROS production and affects the MAPK-HIF-1/NFkB-mediated antioxidant system in Daphnia pulex. Aquat. Toxicol. 220, 105420. https://doi.org/10.1016/j.aquatox.2020.105420.

Liu, L., Xu, K., Zhang, B., Ye, Y., Zhang, Q., Jiang, W., 2021a. Cellular internalization and release of polystyrene microplastics and nanoplastics. Sci. Total Environ. 779, 146523. https://doi.org/10.1016/j.scitotenv.2021.146523.

Liu, S., Shi, J., Wang, J., Dai, Y., Li, H., Li, J., Liu, X., Chen, X., Wang, Z., Zhang, P., 2021b. Interactions between microplastics and heavy metals in aquatic environments: a review. Front. Microbiol. 12, 730. https://doi.org/10.3389/fmicb.2021.652520.

Liu, H.P., Cheng, J., Chen, M.Y., Chuang, T.N., Dong, J.C., Liu, C.H., Lin, W.Y., 2022. Neuromuscular, retinal, and reproductive impact of low-dose polystyrene microplastics on drosophila. Environ. Pollut. 292, 118455. https://doi.org/10.1016/j.envpol.2021.118455.

Ma, Y., Huang, A., Cao, S., Sun, F., Wang, L., Guo, H., Ji, R., 2016. Effects of nanoplastics and microplastics on toxicity, bioaccumulation, and environmental fate of phenanthrene in fresh water. Environ. Pollut. 219, 166–173. https://doi.org/10.1016/j.envpol.2016.10.061.

Maity, S., Biswas, C., Banerjee, S., Guchhait, R., Adhikari, M., Chatterjee, A., Pramanick, K., 2021. Interaction of plastic particles with heavy metals and the resulting toxicological impacts: a review. Environ. Sci. Pollut. Res. 28 (43), 60291–60307. https://doi.org/10.1007/s11356-021-16448-z.

Mendoza, R.P., Brown, J.M., 2019. Engineered nanomaterials and oxidative stress: current understanding and future challenges. Curr. Opin. Toxicol. 13, 74–80. https://doi.org/10.1016/j.cotox.2018.09.001.

Mitrano, D.M., Wick, P., Nowack, B., 2021. Placing nanoplastics in the context of global plastic pollution. Nat. Nanotechnol. 16 (5)), 491–500. https://doi.org/10.1038/s41565-021-00888-2.

Oliveira, P., Barboza, L.G.A., Branco, V., Figueiredo, N., Carvalho, C., Guilhermino, L., 2018. Effects of microplastics and mercury in the freshwater bivalve Corbicula fluminea (Müller, 1774): filtration rate, biochemical biomarkers and mercury bioconcentration. Ecotoxicol. Environ. Saf. 164, 155–163. https://doi.org/10.1016/j.ecoenv.2018.07.062.

Overend, G., Luo, Y., Henderson, L., Douglas, A.E., Davies, S.A., Dow, J.A., 2016. Molecular mechanism and functional significance of acid generation in the drosophila midgut. Sci. Rep. 6 (1), 1–11. https://doi.org/10.1038/srep27242.

Paul, M.B., Stock, V., Cara-Carmona, J., Lisicki, E., Shopova, S., Fessard, V., Braeuning, A., Sieg, H., Böhmert, L., 2020. Micro-and nanoplastics–current state of knowledge with the focus on oral uptake and toxicity. Nanoscale Adv. 2 (10), 4350–4367. https://doi.org/10.1039/D0NA00539H.

Qi, K., Lu, N., Zhang, S., Wang, W., Guan, J., 2021. Uptake of pb (II) onto microplastic associated biofilms in freshwater: adsorption and combined toxicity in comparison to natural solid substrates. J. Hazard. Mater. 411 (6), 125115. https://doi.org/10.1016/j.jhazmat.2021.125115.

Qiao, R., Lu, K., Deng, Y., Ren, H., Zhang, Y., 2019. Combined effects of polystyrene microplastics and natural organic matter on the accumulation and toxicity of copper in zebrafish. Sci. Total Environ. 682, 128–137. https://doi.org/10.1016/j.scitotenv.2019.05.163.

Razanajatovo, R.M., Ding, J., Zhang, S., Jiang, H., Zou, H., 2018. Sorption and desorption of selected pharmaceuticals by polyethylene microplastics. Mar. Pollut. Bull. 136, 516–523. https://doi.org/10.1016/j.marpolbul.2018.09.048.

Rubio, L., Barguilla, I., Domenech, J., Marcos, R., Hernández, A., 2020. Biological effects, including oxidative stress and genotoxic damage, of polystyrene nanoparticles in different human hematopoietic cell lines. J. Hazard. Mater. 398, 122900. https://doi.org/10.1016/j.jhazmat.2020.122900.

Ryan, P.G., Moloney, C.L., 1990. Plastic and other artifacts on south african beaches: temporal trends in abundance and composition. Afr. J. Mar. Sci. 86, 450–452.

Sendra, M., Pereiro, P., Yeste, M.P., Mercado, L., Figueras, A., Novoa, B., 2021. Size matters: zebrafish (Danio rerio) as a model to study toxicity of nanoplastics from cells to the whole organism. Environ. Pollut. 268, 115769. https://doi.org/10.1016/j.envpol.2020.115769.

Silva, A.B., Bastos, A.S., Justino, C.I., da Costa, J.P., Duarte, A.C., Rocha-Santos, T.A., 2018. Microplastics in the environment: challenges in analytical chemistry-a review. Anal. Chim. Acta 1017, 1–19. https://doi.org/10.1016/j.aca.2018.02.043.

Singh, A., Raj, A., Padmanabhan, A., Shah, P., Agrawal, N., 2021. Combating silver nanoparticle-mediated toxicity in Drosophila melanogaster with curcumin. J. Appl. Toxicol. 41 (8), 1188–1199. https://doi.org/10.1002/jat.4103.

Verdú, I., Amariei, G., Plaza-Bolaños, P., Agüera, A., Leganés, F., Rosal, R., Fernández-Piñas, F., 2022. Polystyrene nanoplastics and wastewater displayed antagonistic toxic effects due to the sorption of wastewater micropollutants. Sci. Total Environ. 819, 153063. https://doi.org/10.1016/j.scitotenv.2022.153063.

Viršek, M.K., Lovšin, M.N., Koren, Š., Kržan, A., Peterlin, M., 2017. Microplastics as a vector for the transport of the bacterial fish pathogen species Aeromonas salmonicida. Mar. Pollut. Bull. 125 (1–2), 301–309. https://doi.org/10.1016/j.marpolbul.2017.08.024.

Xu, D., Ma, Y., Han, X., Chen, Y., 2021. Systematic toxicity evaluation of polystyrene nanoplastics on mice and molecular mechanism investigation about their internalization into Caco-2 cells. J. Hazard. Mater. 417, 126092. https://doi.org/10.1016/j.jhazmat.2021.126092.

Zhang, W., Song, K., Ding, R., Han, H., Yao, L., Ji, M., Chen, Z., Yu, H., Wu, C., Fang, T., 2021. Role of polystyrene microplastics in sunlight-mediated transformation of silver in aquatic environments: mechanisms, kinetics and toxicity. J. Hazard. Mater. 419, 126429. https://doi.org/10.1016/j.jhazmat.2021.126429.

Zhao, J., Wang, X., Hoang, S.A., Bolan, N.S., Kirkham, M.B., Liu, J., Xia, X., Li, Y., 2021. Silver nanoparticles in aquatic sediments: occurrence, chemical transformations, toxicity, and analytical methods. J. Hazard. Mater. 418, 126368. https://doi.org/10.1016/j.jhazmat.2021.126368.

Zhou, Q., Yang, N., Li, Y., Ren, B., Ding, X., Bian, H., Yao, X., 2020. Total concentrations and sources of heavy metal pollution in global river and lake water bodies from 1972 to 2017. Glob. Ecol. Conserv. 22, e00925. https://doi.org/10.1016/j.gecco.2020.e00925.

Zhou, D., Cai, Y., Yang, Z., 2022. Key factors controlling transport of micro- and nanoplastic in porous media and its effect on coexisting pollutants. Environ. Pollut. 293, 118503. https://doi.org/10.1016/j.envpol.2021.118503.